

# A peptide derived from melanotransferrin delivers a protein-based interleukin I receptor antagonist across the BBB and ameliorates neuropathic pain in a preclinical model

George Thom<sup>1</sup>, Mei-Mei Tian<sup>2</sup>, Jon P Hatcher<sup>3</sup>, Natalia Rodrigo<sup>1</sup>, Matthew Burrell<sup>1</sup>, Ian Gurrell<sup>3</sup>, Timothy Z Vitalis<sup>4</sup>, Thomas Abraham<sup>5</sup>, Wilfred A Jefferies<sup>6</sup>, Carl I Webster<sup>1</sup> and Reinhard Gabathuler<sup>4</sup>

## Abstract

Delivery of biologic drugs across the blood–brain barrier is becoming a reality. However, the solutions often involve the assembly of complex multi-specific antibody molecules. Here we utilize a simple 12 amino-acid peptide originating from the melanotransferrin (MTf) protein that has shown improved brain delivery properties. 3D confocal fluorescence microscopic analysis demonstrated brain parenchymal localisation of a fluorescently labelled antibody (NIP228) when chemically conjugated to either the MTf peptide or full-length MTf protein. Measurement of plasma kinetics demonstrated the MTf peptide fusions had very similar kinetics to an unmodified NIP228 control antibody, whereas the fusion to MTf protein had significantly reduced plasma exposure most likely due to a higher tissue distribution in the periphery. Brain exposure for the MTf peptide fusions was significantly increased for the duration of the study, exceeding that of the fusions to full length MTf protein. Using a neuropathic pain model, we have demonstrated that fusions to interleukin-I receptor antagonist (IL-1RA) are able to induce significant and durable analgesia following peripheral administration. These data demonstrate that recombinant and chemically conjugated MTf-based brain delivery vectors can deliver therapeutic levels of drug to the central nervous system.

## Keywords

Blood–brain barrier, central nervous system, interleukin-I receptor antagonist, melanotransferrin peptide, pharmacokinetic

Received 31 July 2017; Revised 23 March 2018; Accepted 26 March 2018

## Introduction

Although protective in design, the blood–brain barrier (BBB) presents a constant challenge to effectively deliver therapeutic drugs directed at the treatment of brain diseases. Efficient drug delivery across the BBB is most important in the treatment of neurophysiological disorders (including neuropathic pain, Alzheimer's disease

<sup>4</sup>Bioasis Technologies Inc., Richmond, BC, Canada

<sup>5</sup>Neural and Behavioural Sciences & Microscopy Imaging Core Lab, College of Medicine, The Pennsylvania State University, Hershey, PA, USA

<sup>6</sup>The Michael Smith Laboratories, University of British Columbia, Vancouver, BC, Canada; The Vancouver Prostate Centre, Vancouver General Hospital, Vancouver, BC, Canada; The Djavad Mowafaghian Centre for Brain Health, University of British Columbia, Vancouver, BC, Canada; Centre for Blood Research and Departments of Microbiology and Immunology, Medical Genetics, and Zoology University of British Columbia, Vancouver, BC, Canada

## Corresponding author:

Mei-Mei Tian, Bioasis Biosciences Corp., 14 Water Street, Guilford, CT 06437, USA.

Email: meimei@bioasis.us

<sup>1</sup>MedImmune, Cambridge, UK

<sup>2</sup>Bioasis Biosciences Corp., Guilford, CT, USA

<sup>3</sup>Neuroscience IMED Biotech Unit, AstraZeneca, AKB, Cambridge, UK

and lysosomal storage diseases), brain cancers, trauma and genetic diseases.

Studies have shown that drugs, conjugated to antibodies that bind specific receptors on brain endothelial cells, can cross the BBB. This suggests that using ligands for these receptors as carriers of therapeutic drugs may be of value in facilitating delivery across the brain capillary endothelial cells of the BBB and into the brain.<sup>1–3</sup> However, despite these advances, crossing the BBB remains a key obstacle in the development of drugs for the treatment of brain diseases despite decades of research.<sup>4–6</sup>

One candidate which acts as a carrier for transport across brain capillary endothelial cells is the protein melanotransferrin (MTf), a protein belonging to the transferrin (Tf) family of proteins.<sup>7</sup> Human MTf has been found to share 37–39% protein sequence homology with human serum Tf and human lactotransferrin.<sup>8</sup> Despite this homology, Tf receptor (TfR) has been demonstrated not to be involved in the transcytosis of MTf, but that LDL receptor-related protein-1 (LRP1) may be involved in its transcytosis.<sup>9</sup> In addition, MTf is the only member within the family to exist in two different forms: a membrane protein attached to the cell surface via a glycosylphosphatidylinositol (GPI) anchor and a free soluble form in the serum.<sup>10–13</sup>

The soluble form of MTf has been found to localize on the surface of normal brain endothelial cells, the main constituent of the BBB, and is able to cross through the brain capillary endothelium.<sup>14,15</sup> The soluble form of MTf functions in the transport iron across the BBB.<sup>16</sup> Recombinant human soluble MTf is transported across brain endothelial cells at a rate of 10–15 times higher than Tf in an in vitro model of BBB transcytosis<sup>9,17</sup> and 5.7-fold higher in vivo.<sup>9</sup> It also has the capability to shuttle large molecules across brain endothelial cells. Tang et al.<sup>18</sup> demonstrated that linking soluble MTf to the extracellular domain of the coxsackie-adenovirus receptor was able to re-direct Ad5 vectors to the MTf transcytosis pathway in an in vitro BBB model. Karkan et al.<sup>19</sup> demonstrate that brain delivery of soluble MTf-drug conjugates was quantitatively 10-fold higher than with free drug controls and reduce the growth of brain tumours. Nounou et al.<sup>20</sup> demonstrated that trastuzumab chemically conjugated to MTf reduced the number of preclinical human Her2-positive breast cancer metastases in the brain by 68% compared to control groups, and reduced the size of remaining tumours by 46% compared to control groups. In contrast, trastuzumab alone had no effect on reduction the number of metastases in the brain, and was associated with only a minimal reduction in tumour size.<sup>20</sup>

While MTf therefore offers a potential approach to the transport of drugs to the central nervous system

(CNS), it is a large protein and presents a significant challenge for fusion to biologic drug molecules. In this paper, we describe the utility of a peptide derived from MTf that retains the ability to transcytose across brain endothelial cells, and on fusion to interleukin-1 receptor antagonist (IL-1RA) demonstrates analgesia in a mouse model of neuropathic pain. Brain exposure studies demonstrate that this recombinant MTf peptide-based brain delivery vector is efficient in delivery of therapeutic concentrations of biologics to the CNS.

## Materials and methods

### *The MTf peptide*

The peptide fragment from the trypsin digest of MTf (MTfpep) corresponding to amino acids 441–452 (DSSHAFTLDELRL) of the mature protein was previously identified as crossing the in vitro model of the BBB and is utilized in the current study and details of the identification of the MTf peptide are described elsewhere.<sup>21</sup> Briefly, recombinant human MTf, expressed and purified as previously described by Yang et al.<sup>13</sup> Karkan et al.<sup>19</sup> and Hegedus et al.,<sup>22</sup> was subjected to trypsin digest at 37°C for 20 h and lyophilized. The tryptic peptides were screened with transcytosis assay using the in vitro BBB model (Cellial Technologies, Lens France) using bovine brain capillary endothelial cells grown on collagen-coated polycarbonate transwell inserts (0.4 µm pore size, 24 mm diameter, corning) forming a confluent monolayer supported by primary rat glial cells. Lucifer Yellow (LY) at 20 µM was used as paracellular marker to evaluate the integrity of the cellular barrier. Ringer-HEPES buffer containing the trypsin digest of MTf and LY was placed in the upper chamber (luminal side) of the transwell. The transwells were incubated on a rocking platform at 37°C for 120 min. At the end of the experiment, aliquots were taken from the abluminal and luminal compartments of the transwell and lyophilized and stored at –80°C until mass spectrometry analysis. Samples from the transwell experiment were resolved by liquid chromatography using Agilent Eclipse Plus C18 column. The eluates were analysed on an Agilent 6490 QqQ mass spectrometer in positive mode, controlled by Agilent's MassHunter Workstation software (version B.04.01) and processed using Agilent Quantitation software (version B.04.01).

### *NIP228 hIgG1 control antibody*

NIP228 hIgG1 is a mouse IgG1 kappa monoclonal antibody against 4-hydroxy-3-iodo-5-nitrophenylacetic acid, which is used as a negative control for protein fusion crossing the BBB. When bound to IL-1RA,

it previously showed no analgesia in a mouse model of neuropathic pain as it was not able to cross the BBB.<sup>23</sup>

### **Labelling of the NIP228 antibody and MTF peptide with a fluorescent marker with Alexa Fluor 647 for confocal fluorescence microscopy**

The MTFpep was reacted with Alexa Fluor 647 (AF647) C2-maleimide (Invitrogen A20347) and purified using semi-preparative reverse phase C18 chromatography following the reaction. NIP228 mouse IgG1 antibody was reacted with Alexa Fluor 647 NHS ester (Invitrogen) and then desalted using a Sephadex G-25 column.

### **Chemical conjugation of MTF or MTFpep to NIP228 mAb for confocal fluorescence microscopy**

The Alexa Fluor labelling and conjugation were performed by CellMosaic, Inc. Briefly, desalted NIP228 hIgG1 was reacted with *N*-( $\beta$ -maleimidopropoxy) succinimide ester (BMPS). In a separate reaction, MTF was reacted with 2-pyridyldithiol-tetraoxatetradecane-*N*-hydroxysuccinimide (PEG<sub>4</sub>-SPDP) and then desalted. The fractions collected were subjected to dithiothreitol (DTT) reduction to generate MTF-containing free sulfhydryl groups. Sulfhydryl-containing MTF was further reacted with NIP228 hIgG1 (AF647) containing maleimide groups generated from the mAb (AF647)<sub>n</sub> and BMPS reaction. The reaction was quenched by cysteine, and the crude reaction mixture was purified by size exclusion chromatography. The fractions containing mostly 1:1 MTF and NIP228 hIgG1 conjugate were combined, concentrated and sterilized using a sterile ultrafree MC 0.22  $\mu$ m GV Durapore spin filter. The resulting conjugate contained approx. 2 MTF per NIP228 antibody.

MTFpep-NIP228 hIgG1 conjugate was prepared in similar fashion, where maleimide-containing NIP228 hIgG1 was reacted with thiol-containing MTFpep. The reaction was quenched by cysteine and desalted. The resulting conjugate contained approx. 4 MTFpep per NIP228 antibody.

The conjugation products were analysed by either reversed phase or size exclusion HPLC to determine purity and concentration, and by SDS-PAGE to determine purity and molecular weight.

### **Cloning, expression and purification of MTF and MTFpep-NIP228 fusion constructs**

DNA encoding the amino acid sequence of the V<sub>H</sub> and V<sub>L</sub> of the antibody, NIP228, was assembled by polymerase extension of over-lapping oligonucleotides and cloned into expression vectors containing the

appropriate light or heavy chain constant regions.<sup>24</sup> DNA encoding the entire MTF or MTFpep amino acid sequence (DSSHAFTLDELRL) and (Gly<sub>4</sub>Ser)<sub>2-4</sub> flexible linkers was similarly assembled by polymerase extension of over-lapping oligonucleotides and directional cloning either to the N or C-terminal end of the acceptor IgG heavy chain. All IgGs were expressed as chimeric human IgG1 molecules with the S239D/A330L/I332E triple mutation (IgG1TM).<sup>25</sup> Antibodies were expressed in transiently transfected Chinese hamster ovary (CHO) cells in serum-free media as described previously.<sup>26</sup> Antibodies were purified from cell culture media using protein A affinity chromatography followed by size exclusion chromatography. The concentration of IgG was determined by  $A_{280}$  using an extinction coefficient based on the amino acid sequence of the IgG.<sup>27</sup>

Plasmids enabling the expression of IL-1RA fused to the C-terminus of the IgG1TM heavy chain via a (G<sub>4</sub>S)<sub>3</sub> flexible linker were assembled by PCR amplification of the IL-1RA gene from cDNA obtained from Source Bioscience and subsequent PCR amplification with oligonucleotide primers that overlapped the IL-1RA gene and the IgG1TM CH3 domain and incorporated the linker, described above. Expression and purification of IgG1TM-IL-1RA fusions were performed as previously described.

### **Chemical conjugation of MTFpep-NIP228 mAb constructs**

MTFpep was chemically synthesized with a C-terminal polyethylene glycol (PEG)<sub>4</sub> linker followed by a Lysine residue containing a maleimide grouping for linking to the thiol group of engineered cysteines residues on the Fc region of the NIP228 hIgG1TM as described in Thompson et al.<sup>28</sup> Briefly, to generate the site-specific peptide conjugation, cysteine engineered NIP228 was reduced using 40 molar equivalent excess of TCEP (Tris(2-carboxyethyl) phosphine; Thermo Scientific Bond-breaker TCEP solution) in PBS pH 7.2, 1 mM EDTA (ethylenediaminetetraacetic acid) for 3 h at room temperature. Following buffer exchange to remove TCEP, 20 molar equivalents of dehydroascorbic acid were added for 4 h at room temperature. The resulting solution was filtered through a 0.2- $\mu$ m syringe filter and 10 molar equivalents of MTF peptide were added followed by incubation at room temperature for 1 h. The reaction was quenched by the addition of four equivalents (over MTF peptide) of N-acetyl cysteine. The MTF peptide labelled NIP228 hIgG1TM was purified using size exclusion chromatography. The peptide to antibody ratio was estimated as described in Thompson et al.<sup>28</sup> To avoid differences in renal clearance, molecules containing the MTFpep were

constructed on an IgG, rather than only the Fc domain, as the Fab arms increase the molecular weight and hydrodynamic radius reducing clearance through the kidneys. Figure 1 shows the design and composition of the different molecules based on NIP228, with Figure 1(a) showing the molecules used in peripheral pharmacokinetic (PK) and in brain exposition and Figure 1(b) showing the molecules having integrated IL-1RA on the C terminus of human Fc which were used in the mouse pharmacodynamic (PD) model of neuropathic pain.

### *Brain distribution of MTfpep, mAb and MTfpep/MTf-mAb chemical conjugate by confocal fluorescence microscopy*

The in-life phase and confocal microscopy studies were performed under contract at the National Research Council (NRC) of Canada, (Ottawa, ON). The protocol and procedures involving the care and use of animals in this study were reviewed and approved by Ottawa-NRC Animal Care Committee. The care and use of animals were in accordance with the guidelines of the Canadian Council on Animal Care (CCAC).

The experiments in this study have been reported in compliance with the ARRIVE guidelines (Animal Research: Reporting in Vivo Experiments).

Six-to-eight week old Balb/c female mice ( $n = 3$ ) were injected (i.v.) with mAbAF647 (10 mg/kg), MTf-mAbAF647 (15 mg/kg), and MTfpep-mAbAF647 (10.2 mg/kg), the doses representing equivalent moles/kg doses due to the differing molecular weights of the three molecules. The control groups received vehicle control, phosphate-buffered saline (PBS), or free AF647 (0.1 mg/kg); 2 h post injection, tomato lectin Texas red to label the capillaries (100  $\mu$ g/mouse) was injected (i.v.) prior to euthanasia (10 min). The animals were euthanized by anaesthetisation and perfused with PBS pH 7.4 supplemented with 2.7% BSA, 100 U/mL heparin. The brain was removed, frozen and subjected to cryo-sectioning and immunohistochemistry. Tissue sections were stained with 4',6-diamidino-2-phenylindole (DAPI blue) to label the cell nuclei.

The 3D confocal imaging was performed at the Penn State Hershey College of Medicine Imaging Core Lab. Confocal images of fluorescently labelled cells were acquired with a Leica AOBs SP8 laser scanning confocal microscope (Leica, Heidelberg, Germany) using

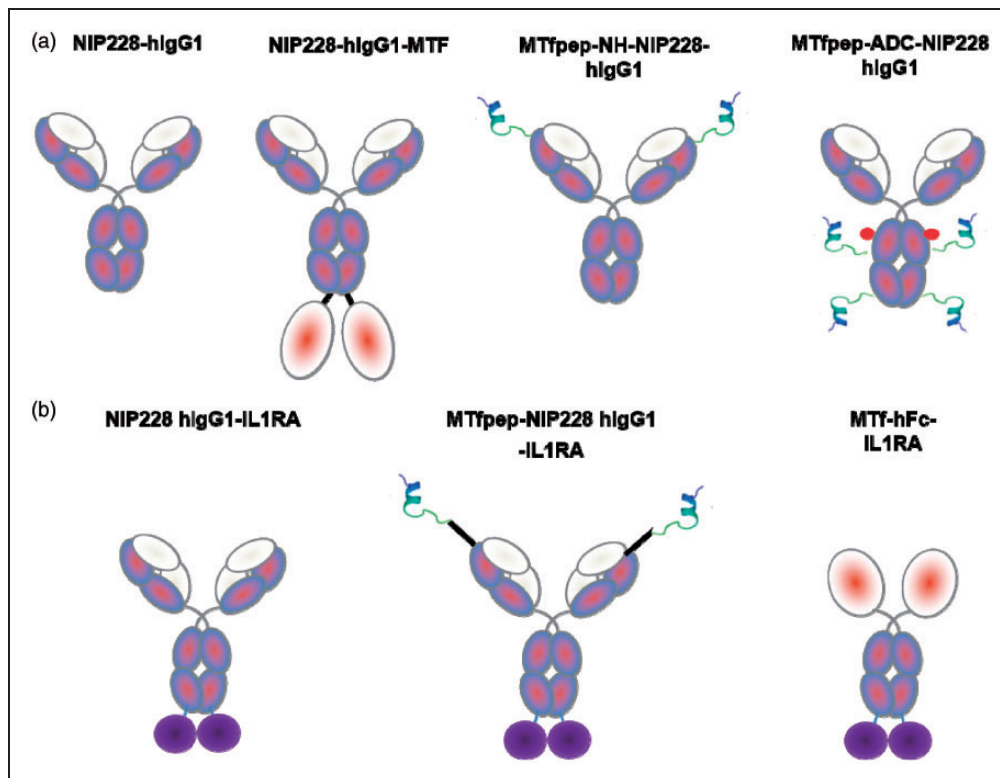


**Figure 1.** Schematic representation of the different molecules studied. In (a), the constructs with NIP228 hlgG1TM antibody alone and incorporating as genetic fusion with flexible linker or chemical conjugation MTf and MTfpep. In (b), the constructs with NIP228hlgG1TM antibody or the Fc fragment of the antibody containing the therapeutic molecule IL-1RA (Kineret) with an analgesic effect and incorporating after genetic fusion MTf or MTfpep with a flexible linker.

a high-resolution Leica 63×/1.4 or 40×/1.3 Plan-Apochromat oil immersion objective lenses. The laser lines used for excitation were continuous wave 405 for DAPI, 80 MHz pulsed 595 nm for Texas Red and 80 MHz pulsed 653 nm for AF647. All images and spectral data (except DAPI) were generated using the highly sensitive Leica HyD hybrid detectors (with time gated option) located inside the scan-head. The 3D stack images with optical section thickness (z-axis) of approximately 0.3 μm were captured from tissue volumes. The 3D image restoration was performed using Imaris software (Bitplane). The volume estimation was performed on the 3D image data sets recorded from five or more different areas of brain tissue samples. Gaussian noise removal filter was applied to define the boundary between foreground and background, and the lower threshold level was set to exclude all possible background voxel values. Sum of all the voxels above this threshold level is determined to be volume. 3D image volume of tissues was systematically compared using similar imaging conditions. Distribution of test articles in brain capillaries and parenchyma is quantified as volume fraction, determined as volume of test article (voxels of AF647 co-localized with either capillary or parenchyma) divided by total tissue volume.

ANOVA multiple comparison analysis used for comparison between the volume fraction of AF647 fluorescence associated with NIP228 hIgG1 and MTfpep-NIP228 hIgG1 or MTf-NIP228 hIgG1 in the brain parenchyma and capillaries. All differences were considered statistically significant at  $p < 0.05$ . Data are reported as mean ± standard deviation (SD).

### Peripheral kinetics and brain exposure

All studies to measure antibody exposure in the periphery and brain were performed at Quotient Biosciences (Newmarket, UK). Male C57Bl/6 mice, age 10–12 weeks were intravenously (i.v.) injected with MTf and the MTfpep genetically or chemically conjugated variants of the control IgG (NIP228) at 20 mg/kg or molar equivalent. Intravenous doses were administered into a tail vein at a constant dose volume of 10 ml/kg. Antibodies were supplied in D-PBS (Sigma). Following dosing, two blood plasma samples were collected into individual Li-Heparin containers from each of six animals per time point (0.08, 2, 4, 6, 8, 24, 48, 96, 120, 168, 240 and 336 h), per dose group. The first sample from each animal was collected from the lateral tail vein (ca 200 μL) into a Li-Hep microvette (BD Diagnostic Systems), while the second sample (ca 600 μL) was collected by cardiac puncture under isoflurane anaesthesia into a Li-hep microtainer (BD Diagnostic Systems). Following collection, blood

samples were allowed to clot for 30 min and centrifuged at 10,000 ×  $g$  for 2 min at 4°C and the resultant plasma drawn off. Plasma samples were flash frozen on dry ice for subsequent analysis. After final blood collection, the mice were perfused with D-PBS at a rate of 2 ml/min for 10 min until the extremities appeared white. Brains were excised, and one hemisphere immediately processed, the other snap frozen in liquid nitrogen.

Brain hemisphere was homogenized in five volumes of ice-cold PBS containing 0.5% Tween 20 and Complete<sup>®</sup> protease inhibitor cocktail tablets (Roche Diagnostics). Homogenisation was performed in a 10 ml Potter-Elvehjem mortar type glass homogeniser with polytetrafluoroethylene (PTFE) pestle, using 2 × 10 clockwise strokes with 5 s rest time. Homogenates were transferred to LoBind tubes (Eppendorf) and rotated at 4°C for 1 h before centrifuging in a chilled bench-top centrifuge at 13,000  $g$  for 20 min. The supernatant was isolated for brain antibody measurement. Five volumes of ice-cold PBS containing 0.2% sodium dodecyl sulphate (SDS) and Complete<sup>®</sup> protease inhibitor cocktail tablets were added to the remaining cell pellet and the pellet processed as described above. The supernatant was again removed and combined with the first supernatant for measurement via MesoScale Discovery (MSD) assay (Meso Scale Diagnostics). MSD multi-array technology enables detection of biomarkers in single and multiplex formats using electrochemiluminescent detection.

Animal husbandry and the procedures used were in accordance with the guidelines of the AstraZeneca Animal Care Committee and complied with the Animals (Scientific Procedures) Act 1986. All experiments were reported in compliance of the Animal Research: Reporting in Vivo Experiments (ARRIVE) guidelines.

### Measurement of antibody concentrations in mouse brain and plasma

Antibody concentrations in mouse plasma and brain samples were measured via MSD assay platform. The MSD assay employs a plate-based sandwich immunoassay format, where anti-human IgG capture antibody binds calibrator or samples, and a specific detection antibody labelled with SULFO-TAG emits light upon electrochemical stimulation. Levels of MTf-NIP228, MTfpep-NIP228 and control antibody alone +/- IL-1RA fusions in plasma and brain samples were quantified by reference to standard curves generated using calibrator samples with a four-parameter non-linear regression model.

Non-compartmental PK analysis (NCA) was performed using Phoenix WinNonlin Professional (version

6.3; Pharsight (Certara), Sunnyvale, CA). Nominal collection times were used for the PK data analyses, with below level of quantification (BLQ) values set to “missing” for calculation of the concentration means at nominal time points. The BLQ values were set as “zero” at pre-dose, and “missing” after peak concentrations for the NCA analysis.

The area under the concentration-time curve to the last measurable time point ( $AUC_{last}$ ) was calculated for plasma and brain using the linear trapezoidal method as implemented in WinNonlin Phoenix. Additionally, systemic clearance (CL), terminal volume of distribution ( $V_z$ ) and terminal half-life ( $t_{1/2}$ ) were determined for plasma. The  $C_{max}$  and  $T_{max}$  quoted are the observed values based on the mean concentration data at each time point.

### Partial nerve ligation

Partial nerve ligation was performed in mice as described in Chessell et al.<sup>29</sup> and Webster et al.<sup>23</sup> In brief, the left sciatic nerve was exposed in female C57Bl/6J mice (Charles River, UK) by blunt dissection through an incision at the level of the mid-thigh. A suture (9/0 Virgin Silk; Ethicon) was then passed through the dorsal third of the nerve and tied tightly. The mice were allowed to recover for at least seven days prior to commencement of testing. Sham-operated mice underwent the same protocol but following exposure of the nerve the mice were allowed to recover. Mice were tested for baseline responses on day 7 and day 10 post surgery. Operated mice showing ipsilateral/contralateral ratios of greater than 80% were classed as non-responders and were removed from the study. The remaining mice were then randomly allocated into treatment groups of 8–10 mice per group with approximately equal ipsilateral/contralateral ratios following which mice were treated with the compound under test. Separate animals were used in each study. All procedures were performed in accordance with the Animals (Scientific Procedures) Act 1986 and were approved by a local ethics committee. Following the establishment of baseline readings, mice were divided into two groups with approximately equal ipsilateral/contralateral ratios which underwent surgery to partially ligate the sciatic nerve or served as sham-operated controls based on the previously described method of Seltzer et al.<sup>30</sup> To investigate the effects of the or MTF or MTfpep fusions, animals received one of PBS vehicle (10 ml/kg bodyweight s.c.) or MTF-hFc-IL-1RA (135 mg/kg s.c.), MTfpep-NIP228-IL-1RA fusion protein (25–100 mg/kg s.c.) or NIP228-IL-1RA (100 mg/kg s.c.). Sham-operated mice received PBS vehicle (10 ml/kg bodyweight s.c.). Mice were re-tested for changes in mechanical hyperalgesia 4h post dose as described

above. Mice were also re-tested at one, two and four days post dose.

### Data analysis

Statistical analysis was performed in GraphPad Prism. Only animals which completed the study were included in the analysis. Results were analysed using two-way ANOVA. Pairwise comparisons, where appropriate, were made using Tukey's test.

## Results

### The MTF BBB transporting peptide

The most efficiently transcytosed peptide, DSSHAFTLDELRL (MTfpep), was previously selected as the candidate for investigating BBB transport *in vivo*. MTfpep is a 12 amino acid peptide located between amino acid 460 to 471 of full length MTF. This peptide is unique to MTF and is not present in other Tf family members such as Tf, lactotransferrin and ovotransferrin. MTfpep sequence differs between rodent species and human by two amino acids, with histidine and alanine at positions 4 and 5 are replaced by tyrosine and serine, respectively, in the rodent species. The two amino acids variation between rodent and human species have no effect on the ability of MTfpep to cross the brain capillary endothelium, nor the ability to transport a payload into the brain and the subsequent efficacy (data not shown).

### *In vivo* brain distribution study of MTF and MTfpep chemically conjugated to fluorescently labeled NIP228

To demonstrate the delivery of an antibody across the BBB *in vivo* using MTF or MTfpep, wild-type mice were injected with conjugates of the control mAb NIP228-AF647 (Figure 2(a)), MTF-NIP228-AF647 (Figure 2(b)) or MTfpep-NIP228-AF647 (Figure 2(c)) via intravenous injection. After 2h post injection, the mice were sacrificed, PBS perfused and brain penetration evaluated and semi-quantified using 3D confocal fluorescence microscopy. Approximately two times greater fractional fluorescence was measured in the brain parenchyma of both MTF-NIP228-AF647 and MTfpep-NIP228-AF647 conjugates compared to NIP228-AF647 alone (Figure 3). More than 95% of the total AF647 fluorescence signal was localized to the brain parenchyma with the remainder localized to the brain capillaries for both MTF-mAb and MTfpep-mAb conjugates. This first step of analysis and experimentation demonstrated that incorporation of MTF or MTfpep increases the transport of a

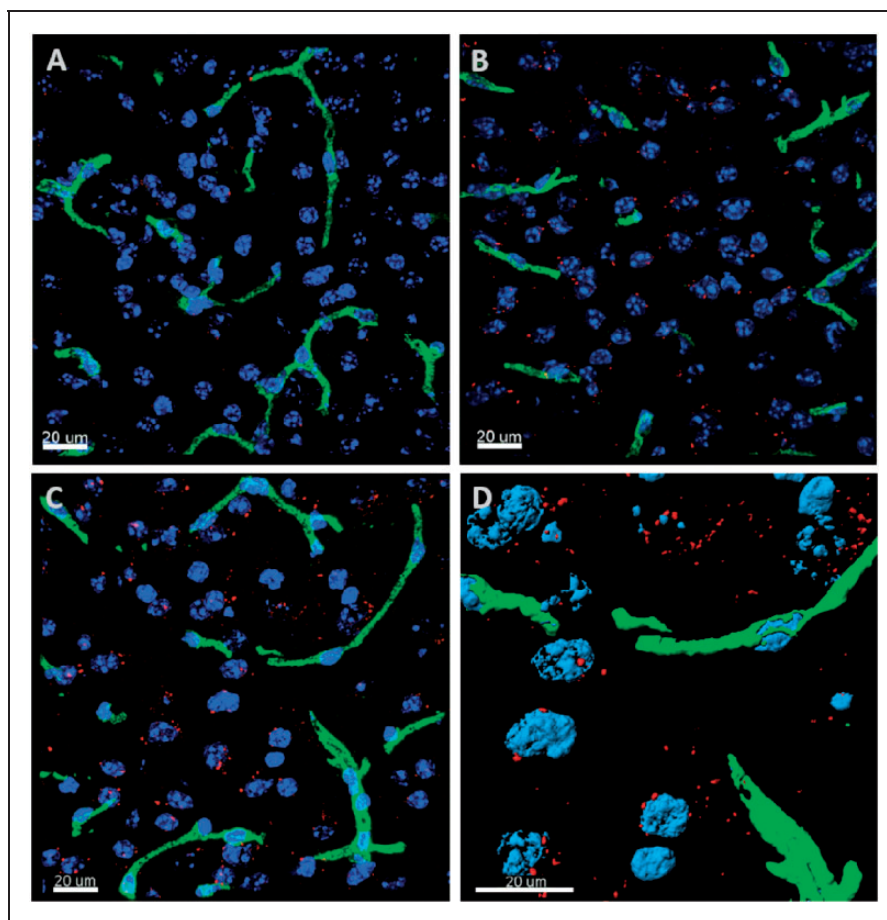


**Figure 2.** Representative 3D confocal image of brain distribution of different constructs based on the mAb NIP228 a hlg1TM 2 h after IV administration in CD-1 female mice. Cell nuclei are blue (DAPI) and capillaries are green (Texas Red). (a) represents the distribution of the NIP228 labelled with Alexa F647 (red); (b) represents the distribution of MTF chemically conjugated to NIP228 labelled with Alexa F647 (red); (c) represents the distribution of MTfpep chemically conjugated to NIP228 labelled with Alexa F647 (red); (d) shows magnified surface rendered (quantified) Texas Red labelled blood capillaries (green) and MTfpep chemically conjugated to NIP228 labelled with Alexa F647 (red). These 3D images demonstrate that the brain parenchyma distribution is much higher for labelled NIP228 incorporating full-length MTF or MTfpep compare to NIP228 alone. See method section for the details of the quantitative procedures. Scale bar represents 20  $\mu\text{m}$ .

mAb through the brain capillary endothelium to the brain parenchyma.

#### *PK properties of fusion and conjugated antibodies after incorporation of MTF or MTfpep*

To confirm that MTF and MTfpep possessed improved brain targeting, we conducted plasma PK and brain exposure studies in C57BL/6J mice. These studies were performed for a period of two weeks, with plasma samples (0.08, 2, 4, 6, 8, 24, 48, 96, 120, 168, 240 and 336 h) and capillary-depleted brain homogenate samples taken at regular intervals (2, 6, 24, 96, 168 and 336 h) throughout that two-week period. The serial sampling procedure in this study resulted in composite profiles for plasma exposure following a single intravenous dose of each of the molecules being tested. All

molecules were dosed at the same molar equivalent (NIP228, MTfpep-NH-NIP228, MTfpep-ADC-NIP228 were dosed at 20 mg/kg, while NIP228-MTF was dosed at 40 mg/kg to compensate for the higher molecular weight of MTF). All parameters were derived using the mean of each data point. Figure 4(a) shows the mean plasma exposure profiles (nM  $\pm$  average deviation) with  $T_{\text{max}}$  achieved at the first-time point (10 min) after intravenous dosing. There is little difference in the plasma PK profiles of the isotype control and the MTfpep constructs, with MTfpep-ADC-NIP228 having a slightly faster clearance value of 14.1 (ml/day/kg) compared to isotype control and the MTfpep genetically fused to NIP228 which possess clearance values of 8 and 5 (ml/day/kg), respectively. However, NIP228-MTF has a significantly altered plasma PK profile, with a much faster clearance rate

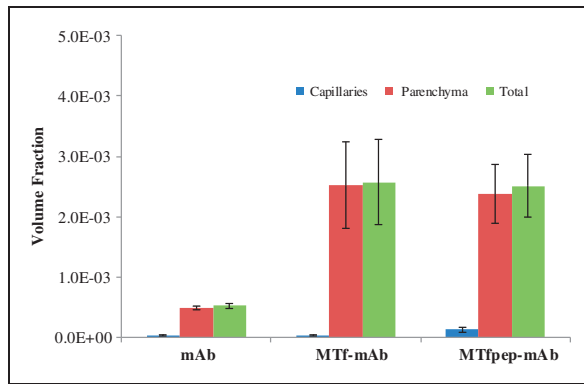


**Figure 3.** Confocal fluorescence microscopy analysis and semi-quantification of the distribution of the different molecules in the brain parenchyma. At 2 h post IV injection, greater than 95% of the MTF-mAb or MTFpep-mAb in the brain is found in the parenchyma rather than the capillary blood vessels. The data clearly show that the molecules containing MTF full-length protein or MTFpep are very efficiently transported across the brain capillary endothelium to the brain parenchyma in Balb/c female mice. Data are reported as mean  $\pm$  standard deviation (SD).

of 74 (ml/day/kg) resulting in a significantly shorter half-life of 5.5 days and a 3-fold lower area under the curve (AUC) when compared to NIP228 control alone (13.8 days) (Supplementary Table 1).

#### **Brain exposure for genetically fused and chemically conjugated antibodies after incorporation of MTF or MTFpep**

Measurement of each of the test molecules in brain homogenate was performed to determine the central exposure. Brain samples were taken from PBS perfused animals at 2, 6, 24, 96, 168 and 336 h post intravenous administration and processed to homogenate for analysis via MSD assay (Figure 4(b)). For both NIP228 and conjugated MTFpep-NIP228 mAbs,  $T_{max}$  occurred at 24 h post administration, while NIP228-MTF conjugated mAb achieved  $T_{max}$  2 h after administration. However, there was a large variation between samples at this time point for NIP228-MTF. NIP228-MTF was below the level of quantification for the assay after 168 h. NIP228 reached  $T_{max}$  four days after administration (Figure 4(b)). MTFpep-conjugated to NIP228 had a significantly prolonged brain exposure when compared to NIP228-MTF and NIP228 alone (Figure 4(b)), with a peak exposure of about 4% of injected dose at the 24-h time point. There was also a significantly higher brain-plasma ratio for both MTFpep-NIP228 conjugated mAbs and NIP228-MTF conjugated mAb, peaking at between 1.5 and 3% at 168 h post administration compared to peak of 0.5% for NIP228 mAb alone (Figure 4(c)).

#### **PK properties for MTF and MTFpep IL-1RA fusion proteins**

Peripheral PK analysis was performed on MTFpep and MTF protein with C-terminal IL-1RA fusions over a two-week period. MTFpep was genetically conjugated with a flexible linker (Gly<sub>4</sub>Ser)<sub>2</sub> to the N-terminal end of the heavy chain of NIP228 and IL-1RA was conjugated to the C-terminal end of the heavy chain of NIP228 with a (Gly<sub>4</sub>Ser)<sub>3</sub> linker. However, MTF protein was genetically conjugated to the N-terminal end of the Fc domain with C-terminal IL-1RA fusion as described above (Figure 1(b)).

Plasma samples were taken at regular intervals throughout the two-week period and processed as described above. NIP228 and MTFpep-NIP228-IL-1RA fusions demonstrated a 4.5 and 7.2-fold reduction in plasma exposure, respectively, as measured by  $AUC_{(last)}$  (Figure 5(a) and Supplementary Table 2) due to a 5–10-fold increased distribution phase ( $V_z$ ) and 9–15-fold increase in clearance (CL) when compared to the plasma exposure of the mAbs without the presence of IL-1RA (Figure 4(a) and Supplementary Table 1). MTF-Fc-IL-1RA  $AUC_{(last)}$  is reduced to 2.3-fold compared to reduction observed for NIP228-MTF; (Figure 5(a) and Supplementary Tables 1 and 2), possibly due to higher clearance rates (CL) for all IL-1RA conjugated mAbs (Supplementary Table 2).  $C_{max}$  for all constructs occurred at the first measured time-point, 10 min post administration.

#### **Brain exposure for MTF and MTFpep IL-1RA fusion proteins**

Brain exposure of the IL-1RA fusions was measured as described above and a composite exposure profile generated (Figure 5(b)).  $T_{max}$  for each molecule tested was at the first measured time point at 2 h, which is somewhat earlier than that observed for the MTFpep-NIP228 and NIP228 constructs without IL-1RA, which were 24 h and 96 h, respectively (Figure 4(b)). Brain exposure of MTFpep-NIP228-IL-1RA and MTF-hFc-IL-1RA was very similar with a maximum exposure of 2.2% injected dose per gram of brain at the first-time point. MTF-hFc-IL-1RA was only detectable in the brain for the first week of the study, after which it was below the lower limit of quantification (LLOQ) for the assay (Figure 5(b)). The lower central exposure of the MTFpep and MTF IL-1RA fusion proteins was possibly due to faster peripheral clearance rates (CL) for the IL-1RA fusions as compared to the MTF fusions lacking IL-1RA.



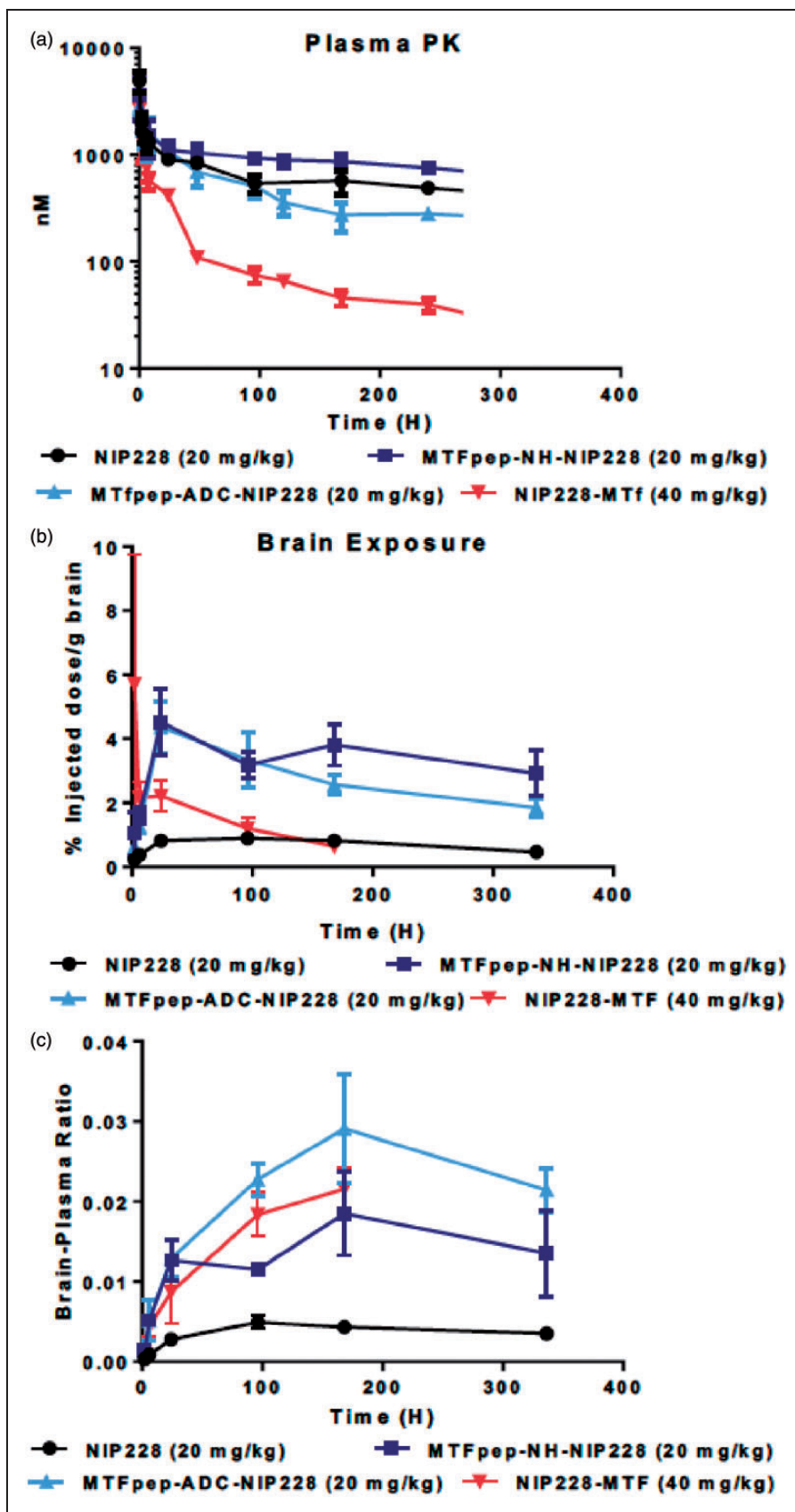


**Figure 4.** Plasma and brain exposure of MTF or MTFpep targeted IgGs in a mouse PK assay. (a) Plasma PK of MTF or MTFpep targeted hlgGITM compared to a non-targeted isotype control (NIP228) over a two-week period. (b) Brain exposure as a measure of % injected dose per gram of brain. (c) Comparison of brain:plasma ratio. All molecules dosed at the same molar concentration. N = 6 per group. PK: pharmacokinetic. S.E.M provided for each measured point indicated.

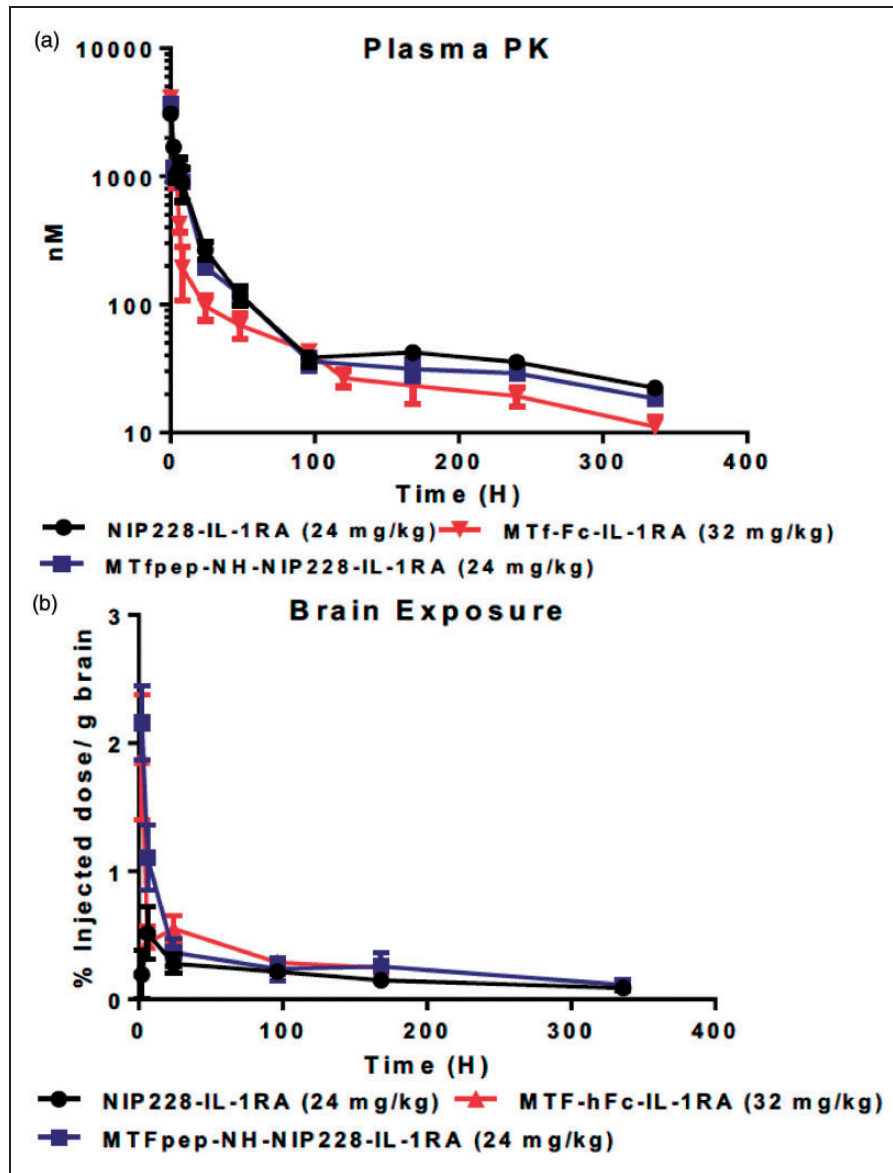


**Figure 5.** Plasma and brain exposure of MTF and MTFpep targeted IgG-IL-1RA fusion molecules in a mouse PK assay. (a) Plasma PK of MTF and MTFpep targeted hlgG fused to IL-1RA compared to a non-targeted isotype control (NIP228) over a two-week period. (b) Brain exposure as a measure of % injected dose per gram of brain. All molecules dosed at the same molar concentration. N = 6 per group. PK: pharmacokinetic; IL-1RA: interleukin 1 receptor antagonist.

### Reversal of mechanical hyperalgesia by BBB transigrating MTF-IL-1RA fusions

Neuropathic pain can be induced by partial ligation of the sciatic nerve in laboratory animals as first described by Seltzer et al.<sup>30</sup> and adapted for mice by Chessell et al.<sup>29</sup> The mechanical hyperalgesia that develops in the model has been shown to be sensitive to the central administration of IL-1RA.<sup>23</sup>

MTF-hFc-IL-1RA or MTFpep (NH or ADC)-NIP228-IL-1RA were administered s.c. at 135 mg/kg or 100 mg/kg, respectively (equimolar dosing) to test

whether mAb-IL-1RA fusions were able to reverse the mechanical hyperalgesia and the mice monitored for four days post dose. No difference in effects was noted between, vehicle, PBS and control mAb-IL-1RA (NIP228-IL-1RA) treated mice indicating NIP228-IL-1RA was not able to access IL-1 receptors in the central compartment (Figure 6(a)). Administration of MTF-hFc-IL-1RA and MTFpep-NIP228-IL-1RA fusions resulted in reversal of mechanical hyperalgesia at time points from 4 h to two days post dose. Only MTFpep (ADC)-NIP228-IL-1RA achieved reversal at four days post dose.

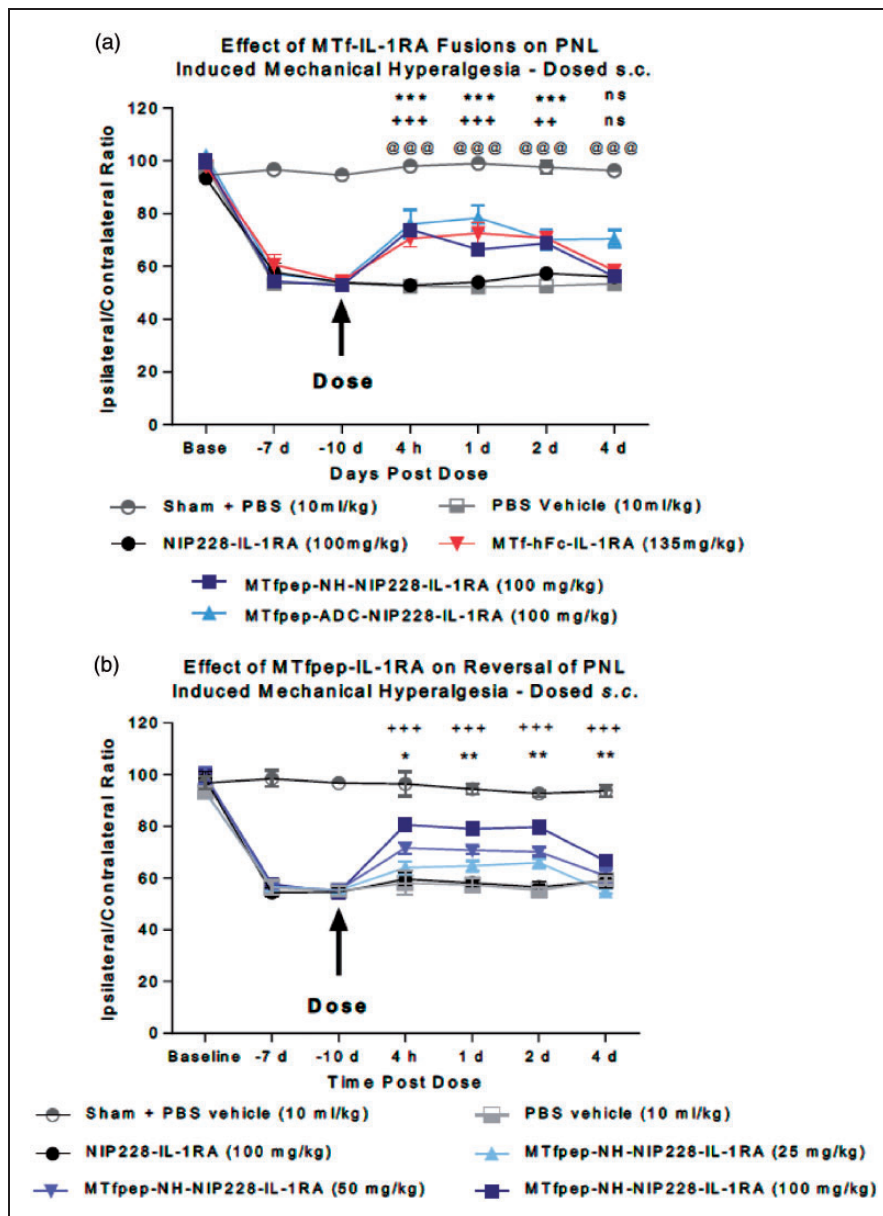


**Figure 6.** The analgesic effect of MTf-IL-1RA fusions on the mouse partial nerve ligation model. (a) Comparison of the analgesic effect of IL-1RA fusion constructs containing MTf and MTfpep with isotype control (NIP228), vehicle control and non-ligated (sham operated) control group. N=8 per group. Data analysed using two-way ANOVA with time and treatment as dependant factors. Subsequent statistical significance obtained using Tukey's POST HOC test. ++  $P < 0.01$ ; +++  $P < 0.001$  – Op + NIP228-IL-1RA vs. Op + MTf-hFc-IL-1RA 135 mg/kg; \*\*\*  $P < 0.001$  – Op + NIP228-IL-1RA vs. Op + MTfpep-NH-NIP228-IL-1RA 100 mg/kg; @@@  $P < 0.001$  – Op + NIP228 vs. Op + MTfpep-ADC-NIP228-IL-1RA 100 mg/kg. (b) Dose response of MTfpep targeted NIP228 hlgITM-IL-1RA fusions on the reversal of partial nerve ligation-induced mechanical hyperalgesia. N=7–10 per group. Data analysed using two-way ANOVA with time and treatment as dependent factors. Subsequent statistical significance obtained using Tukey's post hoc test. \*  $P < 0.05$ ; \*\*  $P < 0.01$  – NIP228 vs. MTfpep 50 mg/kg; +++  $P < 0.001$  – NIP228 vs. MTfpep 100 mg/kg.

The magnitude of the response was very similar for both MTf-hFc-IL-1RA and MTfpep-IL-1RA fusions tested (Figure 6(a)).

To investigate the relationship between dose and the reversal of mechanical hyperalgesia, we administered MTfpep-NH-NIP228-IL-1RA at doses 25, 50 and

100 mg/kg. The different dose levels demonstrated differences in magnitude of the response, but not duration; 50 and 100 mg/kg dosing of MTfpep-NH-NIP228-IL-1RA produced statistically significant analgesic effect compared to NIP228-IL-1RA as analysed using Tukey's post hoc test (Figure 6(b)).

## Discussion

Biologic drugs such as antibodies do not efficiently cross the BBB to elicit an effect in the CNS. However, recent studies have shown that by using receptor-mediated transcytosis, biologics can efficiently reach the brain parenchyma. Delivery of therapeutic antibodies can be achieved by the construction of a form of bispecific antibody, composed of one molecule directed against a brain target and one that target a receptor on the brain endothelial cells for transcytosis,<sup>31</sup> a Fab fragment for transcytosis linked to a therapeutic antibody,<sup>32</sup> or dual-variable domain immunoglobulins, DVD-IgGs.<sup>33</sup> However, these approaches require the assembly of complex bispecific antibody molecules and may present challenges in developing a molecule suitable for the clinic. Peptides binding to specific receptors on the endothelial cells forming the BBB have been used to target biologics to the CNS<sup>34,35</sup> and may offer a more straightforward way of modifying antibodies for transport across the brain capillary endothelium. In this paper, we have described a novel peptide, derived from the sequence of MTF, which, when added to antibodies, is able to facilitate their distribution into the brain.

We have shown that both MTF and a 12 amino-acid peptide derived from MTF (MTfpep) when incorporated in the sequence of a control antibody (NIP228) by chemical conjugation or by genetic fusion can induce the transport of the antibody across the brain capillary endothelium to reach therapeutic concentration in the brain parenchyma. We have used multiple techniques to confirm the brain penetration of antibodies modified with MTF or MTfpep. Using confocal fluorescence microscopy, we were able to visualise an antibody conjugated to MTF or MTfpep labelled with a fluorescent marker, Alexa F647, in the brain parenchyma. Following i.v. administration in mice, the MTF or MTfpep fusions showed a significant increased brain distribution compared to the unconjugated antibody, with 95% of all fluorescence localized in the brain parenchyma (Figures 2 and 3). This observation was confirmed by analysing the concentration of antibodies incorporating MTF and MTfpep in brain homogenate from animals' dosed i.v. (Figure 4(b) and (c)). In this study, MTF was genetically fused to the C-terminus of the antibody heavy chain, and the MTfpep was attached to the antibody either by genetic fusion to the N-terminus of the antibody heavy chain, or by chemical conjugation to the thiol group of an unpaired cysteine introduced into the Fc domain of the antibody. The designs of the different molecules analysed are shown in Figure 1. Brain exposure of the different molecules after i.v. administration was determined following extensive PBS perfusion of the animals, followed by

brain homogenisation. Homogenate was depleted of capillaries in order to determine more accurate amount of molecules present in the brain parenchyma. Molecules containing MTfpep have a significantly prolonged brain exposure when compared to either the MTF containing molecule or the antibody alone (Figure 4(b)). A peak exposure of about 4% of injected dose at the 24-h time point and between 3 and 4% of injected dose for a period of two weeks was observed. This was also reflected in the brain–plasma ratio for both MTfpep- or MTF-NIP228 conjugated or fused proteins compared to NIP228 control antibody alone (Figure 4(c)). Brain–plasma ratio peaks at about 1.5–3% at 168 post administration for the MTfpep or MTF containing proteins compared to 0.5% peak ratio for NIP228 mAb (Figure 4(c)). This study also investigated the plasma PK profiles of these antibodies (Figure 4(a)). The presence of MTfpep on the heavy chains of the antibodies does not affect its plasma PK in contrast to the mAbs containing the MTF protein, which shows a 3-fold shorter peripheral half-life (Supplementary Table 1). This is most likely due to a higher tissue distribution of this construct due to the MTF protein.

To further validate the apparent ability of MTF and MTfpep to deliver molecules into the CNS, pharmacodynamic studies were performed in a mouse model of neuropathic pain. Fusion to IL-1RA enabled measurement of analgesia through a reduction in mechanical hypersensitivity following partial sciatic nerve ligation.<sup>23</sup> The addition of IL-1RA significantly altered the PK of these molecules resulting in a reduction in plasma exposure compared to the equivalent molecule lacking IL-1RA (Figure 5(a) and Supplementary Table 2). This was due to a much-increased distribution phase ( $V_z$ ) and increase in clearance (CL) (Figure 4(a) and Supplementary Table 1), presumably due to IL-1 receptor-mediated clearance. Brain exposure for the IL-1RA fusions was also altered (Figure 5(b)). A peak of exposure is seen at 2 h, which is much earlier than that observed for the MTfpep-NIP228 and NIP228 constructs without IL-1RA (Figure 4(b)). Brain exposure was similar with 2.2% injected dose per gram of brain extracted at the first-time point. The lower central exposure of the MTfpep and MTF IL-1RA proteins was likely due to faster peripheral clearance. In the neuropathic pain model, the control antibody (NIP288) lacking either IL-1RA, MTF, or MTfpep did not induce analgesia (Figure 6(a)). The fusions containing both IL-1RA and either MTF or MTfpep resulted in reversal of mechanical hyperalgesia at time points from 4 h to two days post dose. Only MTfpep chemically conjugated to NIP228-IL-1RA had reversal at four days post dose. The magnitude of

the response was very similar for all MTF-IL-1RA fusions tested (Figure 6(a)). It is of significance to note that the reversal of hyperalgesia was two to four days in length, one day more than if IL-1RA is directly injected intrathecally where the effect lasted one day.<sup>23</sup> This effect was also found to be dose dependent (Figure 6(b)). In addition, we have shown here that our peptide of 12 amino-acid originating from MTF is delivering an analgesic compound (IL-1RA) in the CNS which shows better plasma and brain PK properties than a construct<sup>23</sup> targeting the T<sub>f</sub> receptor by an antibody. While the dose required to achieve analgesia is high, in the absence of more potent analgesics, IL-1RA has enabled this research demonstrating BBB penetration and a pharmacological effect. Future research building on these findings, applying the BBB technology to more efficacious molecules, will assist in the quest to find treatments for neuropathic pain.

In conclusion, we have shown through PK data that MTF and MTFpep are very efficient vectors for the delivery of antibodies across the brain capillary endothelium. Also, as demonstrated in the pharmacodynamic mouse neuropathic pain model, both peptide and full-length protein were able to successfully deliver therapeutic amounts of an analgesic protein IL-1RA fused to an antibody across the BBB into the brain. Aside from being a fraction of the full length MTF in size, this study demonstrated that MTFpep retains the transport capability across brain capillary endothelial cells, with improved PK properties, and has great potential as a delivery platform to transport therapeutic compounds into the brain to treat variety of CNS diseases.

### Funding

The author(s) disclosed receipt of the following financial support for the research, authorship, and/or publication of this article: This work was funded by MedImmune Ltd. and by Bioasis Technologies Inc. TA supported through NIH funding 1S10OD018124-01A1 and 1S10OD010756-01A1. Additional funding for this work was provided to WAJ by grants from the Canadian Institutes for Health Research (MOP-133635), the Natural Sciences and Engineering Research Council of Canada (CRDPJ 452456-13) and an UBC industrial partnership agreement with BiOasis Technologies Inc. (BTI).

### Acknowledgements

The authors thank the National Research Council of Canada for their help in the preparation of tissues to be analysed by confocal fluorescence microscopy and all the staff of MedImmune's Biological Services unit for their invaluable help and technical assistance in performing the mechanical hyperalgesia studies. We thank Dr. Cheryl Pfeifer for her comments on the manuscript.

### Declaration of conflicting interests

The author(s) declared the following potential conflicts of interest with respect to the research, authorship, and/or publication of this article: All MedImmune authors at the time of the work were employees of MedImmune and therefore have a theoretical conflict of interest through being employed by the organisation that both funded the work and may have potential commercial interest in the findings. All BiOasis Technologies Inc. and Bioasis Biosciences Corp. authors at the time of the work were employees of BiOasis and therefore have a theoretical conflict of interest through being employed by the organisation that both funded the work and may have potential commercial interest in the findings. WAJ is the founding scientist of BTI and also acted as a consultant to BTI at the time this work was carried out.

### Authors' contributions

George Thom – Construct creation, PK studies, writing manuscript and directing studies.

Mei-Mei Tian – Directing the work contracted out for the design of labelled construct and determination of the virtual capillary depletion, writing manuscript.

Jon Hatcher – Devising and performing in vivo pharmacodynamic studies.

Natalia Rodrigo – Expression and purification of antibodies.

Matthew Burrell – Expression and purification of antibodies, modification of antibodies with peptides, writing manuscript.

Ian Gurrell – PK data analysis.

Timothy Z Vitalis – Designed experiments and analysis of data that led to the discovery of MTFpep.

Thomas Abraham – Director of Microscopy Imaging at Penn State College of Medicine, directed 3D Fluorescence confocal microscopy and subsequent quantification methods, contributed to writing and editing the manuscript.

Wilfred A Jefferies – Professor at the Michael Smith Laboratories and the Vancouver Prostate Centre at the University of British Columbia provided the recombinant soluble MTF and was involved in the identification, discovery, generation and design of the peptide vector, MTFpep, for brain delivery, commented on the data and assisted in writing the manuscript.

Carl I Webster – Lab PI at MedI, initiated collaboration and generated idea for studies, directed studies and managed work being performed – writing manuscript

Reinhard Gabathuler – Chief Scientist at biOasis, Senior Author, design the experimental approach and identification of the peptide vector, initiated collaboration, managed work being performed, writing manuscript.

### Supplementary material

Supplementary material for this paper can be found at the journal website: <http://journals.sagepub.com/home/jcb>

### References

1. Boado RJ, Zhang Y, Zhang Y, et al. Fusion antibody for Alzheimer's disease with bidirectional transport across the

- blood-brain barrier and A $\beta$  fibril disaggregation. *Bioconjug Chem* 2007; 18: 447–455.
2. Jefferies WA, Brandon MR, Hunt SV, et al. Transferrin receptor on endothelium of brain capillaries. *Nature* 1984; 312: 162–163.
  3. Ueda F, Raja KB, Simpson RJ, et al. Rate of <sup>59</sup>Fe uptake into brain and cerebrospinal fluid and the influence thereon of antibodies against the transferrin receptor. *J Neurochem* 1993; 60: 106–113.
  4. de Boer AG and Gaillard PJ. Drug targeting to the brain. *Annu Rev Pharmacol Toxicol* 2007; 47: 323–355.
  5. Misra A, Ganesh S, Shahiwala A, et al. Drug delivery to the central nervous system: a review. *J Pharm Pharmaceut Sci* 2003; 6: 252–273.
  6. Gabathuler R. Approaches to transport therapeutic drugs across the blood-brain barrier to treat brain diseases. *Neurobiol Dis* 2010; 37: 48–57.
  7. Lambert LA, Perri H and Meehan TJ. Evolution of duplications in the transferrin family of proteins. *Comp Biochem Physiol* 2005; 140: 11–25.
  8. Rose TM, Plowman GD, Teplow DB, et al. Primary structure of the human melanoma-associated antigen p97 (melanotransferrin) deduced from the mRNA sequence. *Proc Natl Acad Sci U S A* 1986; 83: 1261–1265.
  9. Demeule M, Poirier J, Jodoin J, et al. High transcytosis of melanotransferrin (P97) across the blood-brain barrier. *J Neurochem* 2002; 83: 924–933.
  10. Alemany R, Vila MR, Franci C, et al. Glycosyl phosphatidylinositol membrane anchoring of melanotransferrin (p97): apical compartmentalization in intestinal epithelial cells. *J Cell Sci* 1993; 104(Pt 4): 1155–1162.
  11. Food MR, Rothenberger S, Gabathuler R, et al. Transport and expression in human melanomas of a transferrin-like glycosylphosphatidylinositol-anchored protein. *J Biol Chem* 1994; 269: 3034–3040.
  12. Brown DA and Rose JK. Sorting of GPI-anchored proteins to glycolipid-enriched membrane subdomains during transport to the apical cell surface. *Cell* 1992; 68: 533–544.
  13. Yang J, Tiong J, Kennard M, et al. Deletion of the GPI pre-anchor sequence in human p97 – a general approach for generating the soluble form of GPI-linked proteins. *Protein Expr Purif* 2004; 34: 28–48.
  14. Rothenberger S, Food MR, Gabathuler R, et al. Coincident expression and distribution of melanotransferrin and transferrin receptor in human brain capillary endothelium. *Brain Res* 1996; 712: 117–121.
  15. Yamada T, Tsujioka Y, Taguchi J, et al. Melanotransferrin is produced by senile plaque-associated reactive microglia in Alzheimer's disease. *Brain Res* 1999; 845: 1–5.
  16. Moroo I, Ujiie M, Walker BL, et al. Identification of a novel route of iron transcytosis across the mammalian blood-brain barrier. *Microcirculation* 2003; 10: 457–462.
  17. Desrosiers RR, Bertrand Y, Nguyen Q-T, et al. Expression of melanotransferrin isoforms in human serum: relevance to Alzheimer's disease. *Biochem J* 2003; 374: 463–471.
  18. Tang Y, Han T, Everts M, et al. Directing adenovirus across the blood-brain barrier via melanotransferrin (P97) transcytosis pathway in an in vitro model. *Gene Ther* 2007; 14: 523–532.
  19. Karkan D, Pfeifer C, Vitalis TZ, et al. A unique carrier for delivery of therapeutic compounds beyond the blood-brain barrier. *PLoS One* 2008; 3: e2469.
  20. Nounou MI, Adkins CE, Rubinchik E, et al. Anti-cancer antibody trastuzumab-melanotransferrin conjugate (BT2111) for the treatment of metastatic HER2+ breast cancer tumors in the brain: an in-vivo study. *Pharm Res* 2016; 33: 2930–2942.
  21. Eyford BA, Abraham T, Munro L, et al. A peptide vector delivers siRNA across the blood-brain barrier resulting in attenuation of ischemic stroke. In revision. *Nature Biomed Eng*.
  22. Hegedus DD, Pfeifer TA, Theilmann DA, et al. Differences in the expression and localization of human melanotransferrin in lepidopteran and dipteran insect cell lines. *Protein Expr Purif* 1999; 15: 296–307.
  23. Webster CI, Hatcher J, Burrell M, et al. Enhanced delivery of IL-1 receptor antagonist to the central nervous system as a novel anti-transferrin receptor-II-1RA fusion reverses neuropathic mechanical hypersensitivity. *Pain* 2017; 158: 660–668.
  24. Persic L, Roberts A, Wilton J, et al. An integrated vector system for the eukaryotic expression of antibodies or their fragments after selection from phage display libraries. *Gene* 1997; 187: 9–18.
  25. Oganessian V, Gao C, Shirinian L, et al. Structural characterization of a human Fc fragment engineered for lack of effector functions. *Acta Crystallogr Sect D Biol Crystallogr* 2008; 64: 700–704.
  26. Daramola O, Stevenson J, Dean G, et al. A high-yielding CHO transient system: coexpression of genes encoding EBNA-1 and GS enhances transient protein expression. *Biotechnol Prog* 2014; 30: 132–141.
  27. Pace CN, Vajdos F, Fee L, et al. How to measure and predict the molar absorption coefficient of a protein. *Protein Sci* 1995; 4: 2411–2423.
  28. Thompson P, Fleming R, Bezabeh B, et al. Rational design, biophysical and biological characterization of site-specific antibody-tubulysin conjugates with improved stability, efficacy and pharmacokinetics. *J Control Release* 2016; 236: 100–116.
  29. Chessell IP, Hatcher JP, Bountra C, et al. Disruption of the P2X7 purinoceptor gene abolishes chronic inflammatory and neuropathic pain. *Pain* 2005; 114: 386–396.
  30. Seltzer Z, Dubner R and Shir Y. A novel behavioral model of neuropathic pain disorders produced in rats by partial sciatic nerve injury. *Pain* 1990; 43: 205–218.
  31. Yu YJ, Zhang Y, Kenrick M, et al. Boosting brain uptake of a therapeutic antibody by reducing its affinity for a transcytosis target. *Sci Transl Med* 2011; 3: 84ra44.
  32. Niewoehner J, Bohrmann B, Collin L, et al. Increased brain penetration and potency of a therapeutic antibody using a monovalent molecular shuttle. *Neuron* 2014; 81: 49–60.

33. Jakob CG, Edalji R, Judge RA, et al. Structure reveals function of the dual variable domain immunoglobulin (DVD-Ig<sup>TM</sup>) molecule. *MAbs* 2013; 5: 358–363.
34. Regina A, Demeule M, Tripathy S, et al. ANG4043, a novel brain-penetrant peptide-mAb conjugate, is efficacious against HER2-positive intracranial tumors in mice. *Mol Cancer Ther* 2015; 14: 129–40.
35. Webster CI, Caram-Salas N, Haqqani AS, et al. Brain penetration, target engagement, and disposition of the blood-brain barrier-crossing bispecific antibody antagonist of metabotropic glutamate receptor type 1. *FASEB J* 2016; 30: 1927–1940.